Fractal image analysis: application to the topography of Oregon and synthetic images

Jie Huang and Donald L. Turcotte

Department of Geological Sciences, Cornell University, Ithaca, New York 14853

Received January 2, 1990; accepted February 12, 1990

The Earth's topography generally obeys fractal statistics; after either one- or two-dimensional Fourier transforms the amplitudes have a power-law dependence on wave number. The slope gives the fractal dimension, and the unit wave-number amplitude is a measure of the roughness. In this study, digitized topography for the state of Oregon (~7 points/km) has been used to obtain maps of fractal dimension and roughness amplitude. The roughness amplitude correlates well with variations in relief and is a promising parameter for the quantitative classification of landforms. The spatial variations in fractal dimension are low and show no clear correlation with different tectonic settings. For Oregon the mean fractal dimension from a two-dimensional spectral analysis is $D = 2.586$, and for a one-dimensional spectral analysis the mean fractal dimension is $D = 1.487$, which is close to the Brown noise value $D = 1.5$. Synthetic two-dimensional images have also been generated for a range of D values. For $D = 2.6$, the synthetic image has a mean one-dimensional spectral fractal dimension $D = 1.58$, which is consistent with our results for Oregon. This approach can be easily applied to any digitized image that obeys fractal statistics.

INTRODUCTION

The concept of fractals was introduced by Mandelbrot[1] as a measure of the Earth's topography, the length of a rocky coastline. Mandelbrot[2] subsequently obtained a synthetic topography by using fractal statistics that were remarkably realistic. The applicability of fractal concepts to the Earth's topography should not be surprising since it requires only scale invariance, and it has long been recognized that topography is scale invariant in a variety of geological terrains. One of the first things that geology students are taught is the necessity of placing an object, e.g., a coin or person, in a photograph of a geological scene; otherwise it is impossible to tell the scale. It has been observed that the Earth's topography is generally scale invariant for wavelengths from 10^3 to 0.1 km.

The Earth's topography is a composite of many competing influences. Topography is created by tectonic processes including faulting, folding, and flexure; it is modified and destroyed by erosion and sedimentation. Some aspects of topography are deterministic; the flexure of the elastic lithosphere is an example. Flexure introduces a characteristic length of several hundred kilometers to topography, and this length is associated with the structure of many sedimentary basins. However, much of the Earth's topography is complex and chaotic; young mountain ranges are an example. There is also strong evidence that erosional processes lead to complex and chaotic topography. Yet there is order in the chaos of topography, as shown by the applicability of fractal statistics; this order is the result of scale invariance.

The primary purpose of this paper is to illustrate the concept of fractal mapping of digitized images; to do this we consider the digitized topography of the state of Oregon. We first show that the topography of the state satisfies fractal statistics to a good approximation. We then use the fractal dimensions and roughness amplitudes from subregions to construct maps of these quantities for the entire state. This approach can be used for the study of any digitized set of data that obeys fractal statistics.

FRACTAL STATISTICS

The definition of a fractal set is given by

$$N_i = C/r_i^D, \tag{1}$$

where N_i is the number of objects with a linear dimension r_i, D is the fractal dimension, and C is a constant of proportionality. A generalization of Eq. (1) for a continuous distribution is

$$N = C/r^D, \tag{2}$$

where N is the number of objects with a linear dimension greater than r. A wide variety of physical phenomena are found empirically to satisfy Eq. (1) or (2). Examples in the earth sciences include Korcak's empirical relation for the number of islands with an area A greater than a specified values,[3] Rosin's law for number–size distribution of rock fragments,[4] and the Gutenberg–Richter frequency–magnitude relationship for earthquakes.[5]

The fractal definition [Eq. (1)] can be applied to the length of a trail or the perimeter of an object as a function of the step length. If the step length is r_i and the number of steps is N_i, the length of the perimeter P_i is given by

$$P_i = N_i r_i = C r_i^{1-D}. \tag{3}$$

Mandelbrot[1] showed in his paper introducing the term fractal that the length of the west coast of Great Britain satisfies Eq. (3) with $D = 1.25$. This method can be used to determine the fractal dimension of a terrain from the length of a contour on a topographic map as a function of the step length. In mountainous areas, good agreement with Eq. (3) is generally found, and $1.15 < D < 1.30$.[6] There is little or no correlation of the D value with tectonic style or geological

0740-3232/90/061124-07$02.00

age. It should be emphasized, however, that not all regions yield well-defined fractal dimensions[7]; young volcanic islands are an example. The applicability of either Eq. (1) or (2) to a real data is generally over a limited range of scales. This range suggests the range of applicability of the scale-invariant physics. In some cases the data will yield different fractal dimensions over different ranges of scales. This is evidence for the applicability of different scale-invariant physical processes.

Topography can also be used to illustrate the differences between self-similar and self-affine fractals. Studies of topography involving two horizontal coordinates yield self-similar fractals. This is because the two horizontal coordinates are statistically indistinguishable. Examples include number–area statistics for islands and length-of-perimeter statistics. However, because of the asymmetric influences of gravity and other physical processes, the height of topography is not self-similar to the two horizontal coordinates. The relief of topography h along a linear track is an example of a self-affine fractal, and Fourier spectral analysis is a widely accepted approach to the quantification of the fractal dimension.

One-Dimensional Spectral Method

For a self-affine fractal the spectral energy density S of the profile must have a power-law dependence on wave number k (Ref. 8):

$$S(k) \sim k^{-\beta}. \tag{4}$$

In order to relate the power-law dependence of the spectra to the fractal dimension, we consider the specific example of a one-dimensional topographic profile $h(x)$. The variance V is defined by

$$V(L) = \frac{1}{L}\int_0^L [h(x) - \bar{h}]^2 dx, \tag{5}$$

where L is the length over which the profile is specified and $\bar{h}$ is the mean elevation over this length. A necessary condition that the profile be a fractal is that the variance $V(L)$ must have a power-law dependence on the length L (Refs. 9, 10):

$$V(L) \sim L^{2H}. \tag{6}$$

The standard deviation is related to the length of the profile L by

$$\sigma(L) = [V(L)]^{1/2} \sim L^H. \tag{7}$$

For fractional Brownian motion, H is in the range $0 < H < 1$. In order to define the relevant fractal dimension, we introduce a reference box with a width L and a height σ.[9] If the fractal were self-similar, the box would be square; however, for self-affine fractals, arbitrary rectangular boxes must be used. Consider a set of nth-order-smaller boxes with width $L_n = L/n$ and height $h_n = \sigma/n$; n is an integer. The number of nth-order boxes N_n required to cover a width L and a height $\sigma_n = \sigma(L/n)$ is

$$N_n = \frac{L\sigma_n}{L_n h_n} = n^2 \frac{\sigma_n}{\sigma}, \tag{8}$$

and, using relation (7), we find that

$$\frac{\sigma_n}{\sigma} = \frac{\sigma(L/n)}{\sigma(L)} = \frac{1}{n^H}, \tag{9}$$

and, combining Eqs. (8) and (9), we have

$$N_n = n^{2-H} = (L/L_n)^{2-H}. \tag{10}$$

Comparing Eq. (10) with the definition of the fractal dimension in Eq. (1), we have

$$D = 2 - H. \tag{11}$$

The spectral energy density $S(L)$ will also have a power-law dependence on the length L and can be related to the variance $V(L)$ by[10]

$$S(L) = LV(L) \sim L^\beta \sim L^{1+2H}, \tag{12}$$

so that

$$D = \frac{5-\beta}{2}. \tag{13}$$

For a one-dimensional profile, D is expected to lie in the range $1 < D < 2$; the corresponding range for β is $3 > \beta > 1$. For Brown noise $\beta = 2$, $H = 0.5$, and $D = 1.5$.

A number of authors have carried out one-dimensional Fourier-transform studies of topography and bathymetry.[11–18] These studies have found a good correlation with relation (4) with $\beta = 2$ ($D = 1.5$) for wavelengths from 10^3 to 0.1 km; topography appears to be Brown noise. The implications of this observation have been discussed by Bell.[4] For Brown noise the amplitude is proportional to the wavelength; in this sense, topography is truly self-similar. The topography of the Earth as a whole can be expanded in terms of spherical harmonics.[19] Turcotte[20] has shown that the spectral energy density for this correlation also satisfies relation (4) with $\beta = 2$ ($D = 1.5$).

Two-Dimensional Spectral Method

The Fourier spectral approach of fractal analysis for one-dimensional profiles discussed in the previous section can be extended to two-dimensional image analysis. Consider an $N \times N$ grid of equally spaced data points in a square with linear size L, so that the grid spacing is L/N. The N^2 data points are denoted by h_{nm}, with n and m specifying the position in the x and y directions, respectively.

The first step is to carry out a two-dimensional discrete Fourier transform on the N^2 set of h_{nm} data points. An $N \times N$ array of complex coefficients H_{st} is obtained by the usual definition:

$$H_{st} = \sum_{n=0}^{N-1}\sum_{m=0}^{N-1} h_{nm} \exp\left[-\frac{2\pi i}{N}(sn + tm)\right], \tag{14}$$

where s denotes the transform in the x direction ($s = 0, 1, 2, \ldots, N-1$) and t denotes the transform in the y direction ($t = 0, 1, 2, \ldots, N-1$). Then each transform coefficient H_{st} is assigned an equivalent radial number by using the relation

$$r = (s^2 + t^2)^{1/2}. \tag{15}$$

The two-dimensional mean spectral energy density S_{2j} for each radial wave number k_j is given by

$$S_{2j} = \frac{L^2}{N_j}\sum_1^{N_j} |H_{st}|^2, \tag{16}$$

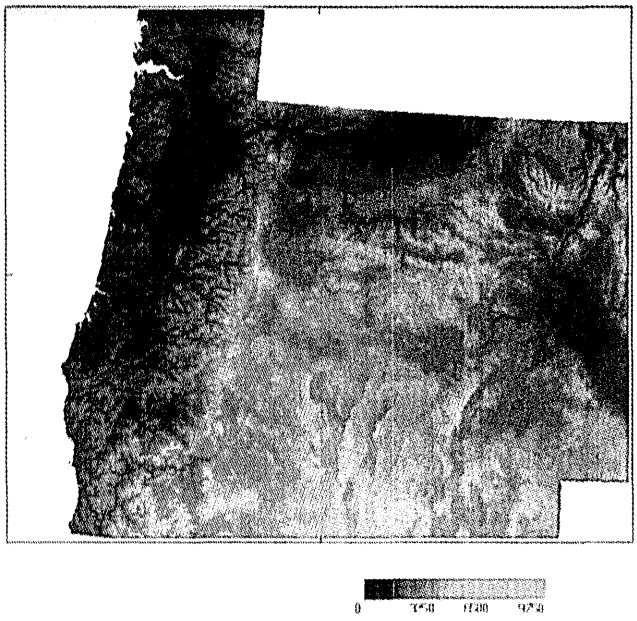

Fig. 1. Gray-scale map of the digitized topography for Oregon. The data resolution is ~7 points/km.

where N_j is the number of coefficients that satisfy the condition $j < r < j + 1$ and the summation is carried out over the coefficients H_{st} in this range.

The two-dimensional equivalent of relation (4) is[21]

$$S_{2j} \sim k_j^{-1-\beta}. \tag{17}$$

The additional power of k_j is required because of the radial coordinates that are used in phase space. The dependence of $V(L)$ on L given in relation (6) is still valid, but, with the additional dimension, the box derivation that follows now gives

$$D_2 = 3 - H \tag{18}$$

instead of Eq. (11) for the fractal dimension of the surface.

For the two-dimensional spectral energy density we have

$$S_2(L) \sim L^2 V(L) \sim L^{1+\beta} \sim L^{2+2H}, \tag{19}$$

so that

$$D_2 = \frac{7-\beta}{2} \tag{20}$$

for the two-dimensional case.

DATA ANALYSIS

One-Dimensional Analysis

As a specific example, we will consider digitized topography for the state of Oregon (Fig. 1). Combining Defense Mapping Agency 1 deg × 1 deg data with topographic maps, the U.S. Geological Survey (Flagstaff) has produced digitized topography on a grid scale of ~7 points/km. We have previously used this technique to study the topography of Arizona.[22]

In order to examine the fractal behavior of the data, one-dimensional spectral analyses are carried out first on three areas with different geomorphic and tectonic settings. The Willamette lowland is dominated by sedimentary processes,

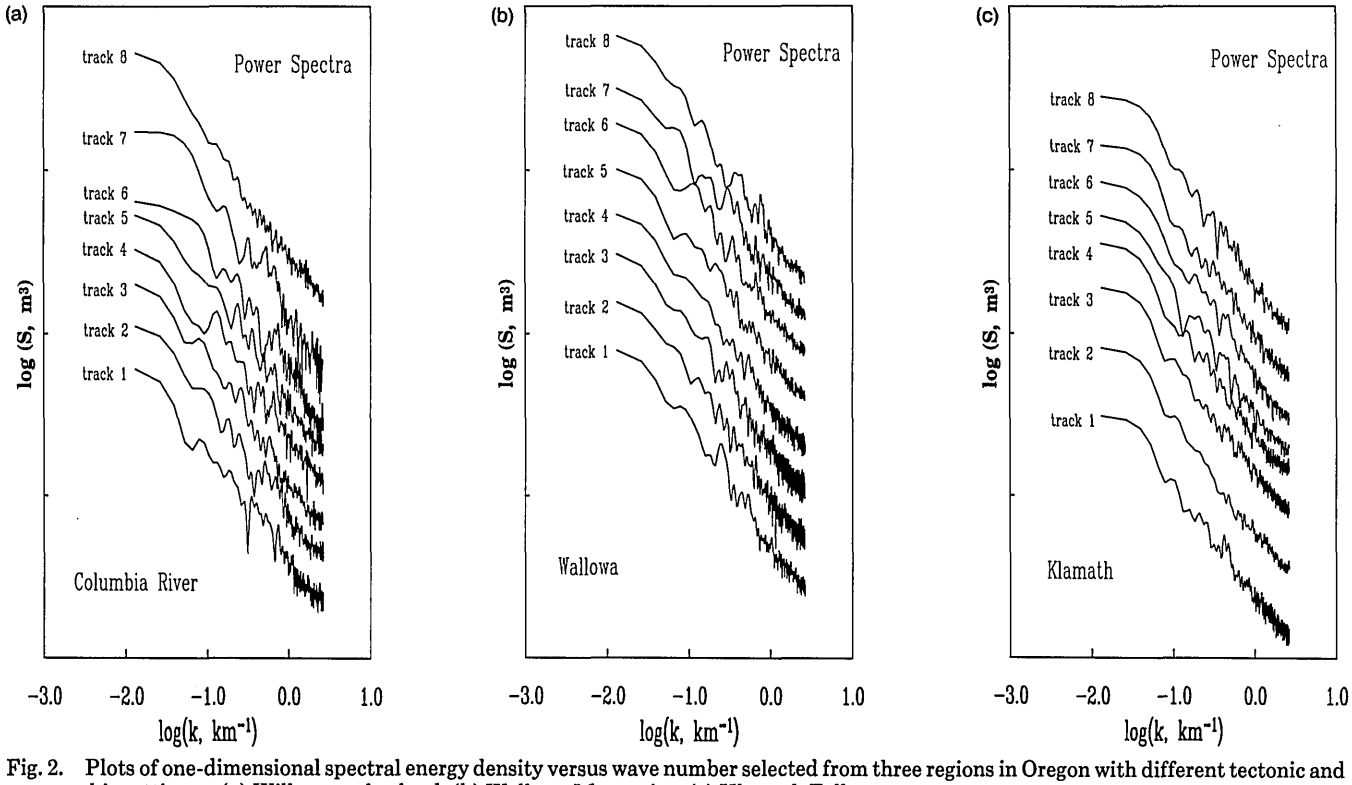

Fig. 2. Plots of one-dimensional spectral energy density versus wave number selected from three regions in Oregon with different tectonic and geomorphic settings: (a) Willamette lowland, (b) Wallowa Mountains, (c) Klamath Falls.

Table 1. Regional Averages over One-Dimensional Profiles of Oregon Topography

Area	Dimension	Roughness	Root Mean Square
Willamette Lowland			
latitude	1.436	5.948	0.205
longitude	1.507	6.354	0.182
Wallowa Mountains			
latitude	1.499	6.549	0.163
longitude	1.485	6.830	0.166
Klamath Falls			
latitude	1.492	5.825	0.178
longitude	1.500	5.963	0.170

the Wallowa Mountains are associated with a major tectonic uplifting, and the Klamath Falls area belongs to the basin and range tectonic regime. For each of the three regions, 20 equally spaced one-dimensional profiles of length 512 are analyzed in both the latitudinal and longitudinal directions. One-dimensional Fourier spectral analyses are performed on them by using the classical periodogram approach. Log–log plots of the spectral energy density versus wave number show a good power-law dependence in all three regions (Fig. 2), which indicates fractal behavior. The average one-dimensional fractal dimensions shown in Table 1 are close to $D = 1.5$, and the small variation in the values in the two perpendicular directions suggest that the Oregon topography is relatively isotropic.

Fractal Mapping of Oregon

The fact that fractal statistics is a good approximation for topography that has been shown in the last section permits us to make fractal maps of a region of diverse tectonics. Using digitized topography of Oregon, we can make plots of spectral density versus wave number for subregions. From these plots a fractal dimension (slope) and unit wave-number amplitude will be obtained from each subregion. The amplitude is a measure of roughness. We are basically carrying out a texture analysis, using the fractal statistics as a basis.

In this study, fractal dimensions and roughness amplitudes will be obtained by using subregions of 32 × 32 data points. Thus fractal dimensions and roughness amplitudes will be obtained for each 4.5 × 4.5-km subregion in the state; maps are generated. We have also carried out studies by using square subregions with 16 × 16 and 64 × 64 data points. The 32 × 32 set was chosen because it generally gives well-defined fractal spectra; for the smaller regions the errors in fractal dimension and roughness become substantially larger. For larger regions, the spatial resolution of the map is degraded.

The following technique is used to obtain a fractal dimension and roughness amplitude for each subregion:

(1) A 32 × 32 set of digitized elevations is chosen to form each subregion ($N = 32$).

(2) The mean and linear trends for each subset of data are removed.

(3) A two-dimensional discrete Fourier transform is carried out, and an $N \times N$ array of complex Fourier coefficients H_{st} is obtained by using Eq. (14).

(4) Each coefficient H_{st} is assigned an equivalent radial wave number r by using Eq. (15). The two-dimensional mean spectral energy density S_{2j} is obtained for each radial integer wave number k_j by using Eq. (16).

(5) The mean slope on a log–log plot of S_{2j} versus k_j obtained by a least-squares regression yields a fractal dimension D_2 by using relations (17) and (20); the intercept at $k_j = 1$ cycle/km yields a roughness amplitude.

Examples for four randomly selected subregions in Oregon are given in Fig. 3. The mean two-dimensional fractal dimension for all of Oregon is $D_2 = 2.586$ (Table 2). This value is remarkably close to the mean value $D_2 = 2.59$, which we previously obtained for the state of Arizona. It is seen that our results are in good agreement with the relation $D_2 = 1 + D$.

Maps of fractal dimension and roughness amplitude are given in Figs. 4(a) and 4(b), respectively. As expected, there is relatively little variation in the fractal dimension about the mean value, although the range is approximately $2.40 < D < 2.90$. The variation in the roughness amplitude in Fig.

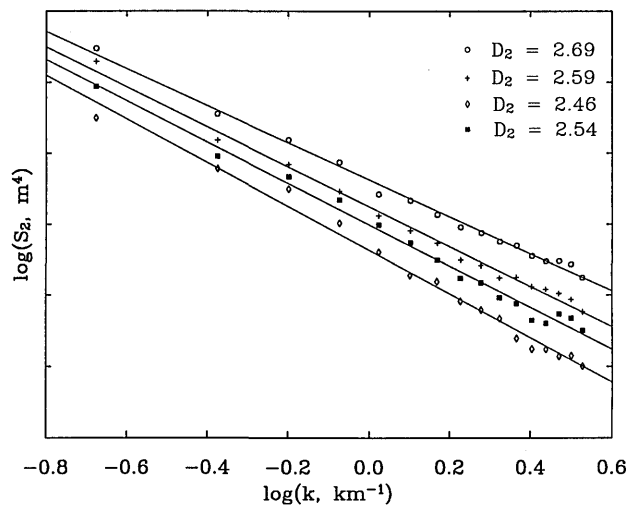

Fig. 3. Plots of mean spectral energy density versus radial wave number for four typical 32 × 32 point subregions in Oregon. The linear trend on a log–log plot indicates a power-law fractal distribution.

Table 2. Summary of Mean Fractal Dimensions Estimated by One-Dimensional and Two-Dimensional Spectral Analysis for Both the Topography of Oregon and Synthetic Images

	Two-Dimensional Analysis		One-Dimensional Analysis	
Data	Average D	Standard Deviation	Average D	Mean Root Mean Square
Oregon Topography	2.586	0.123	1.487	0.149
Synthetic Topography	2.60	—	1.58	0.167
	2.70	—	1.65	0.192
	3.00	—	1.91	0.205

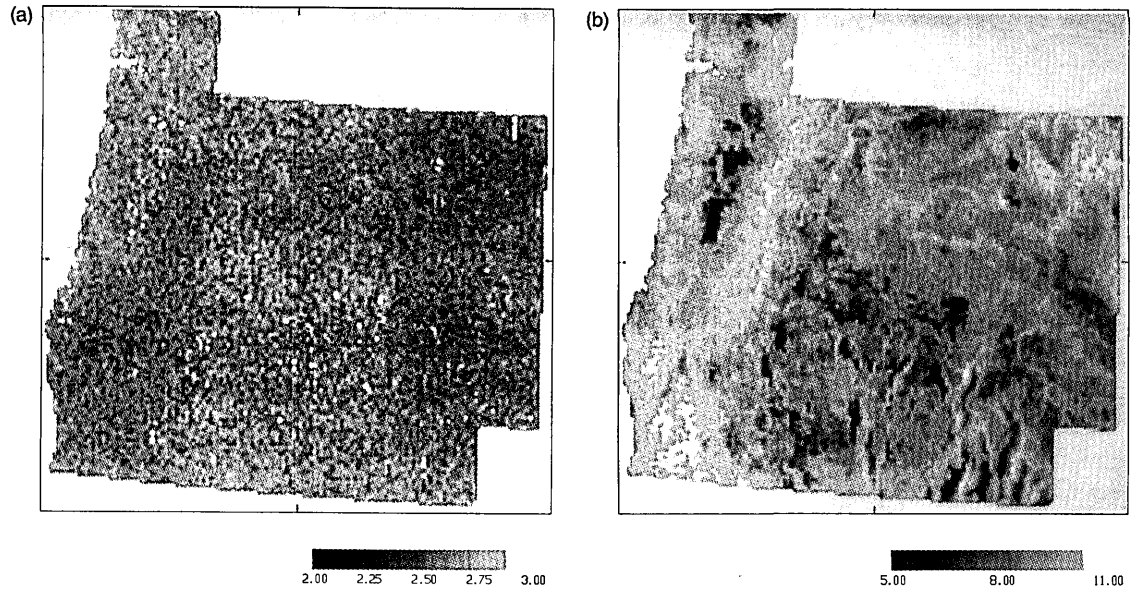

Fig. 4. Gray-scale maps for Oregon: (a) fractal dimension, (b) roughness amplitude. There is generally limited systematic variation in the fractal dimension; however, the roughness amplitude is sensitive to texture changes.

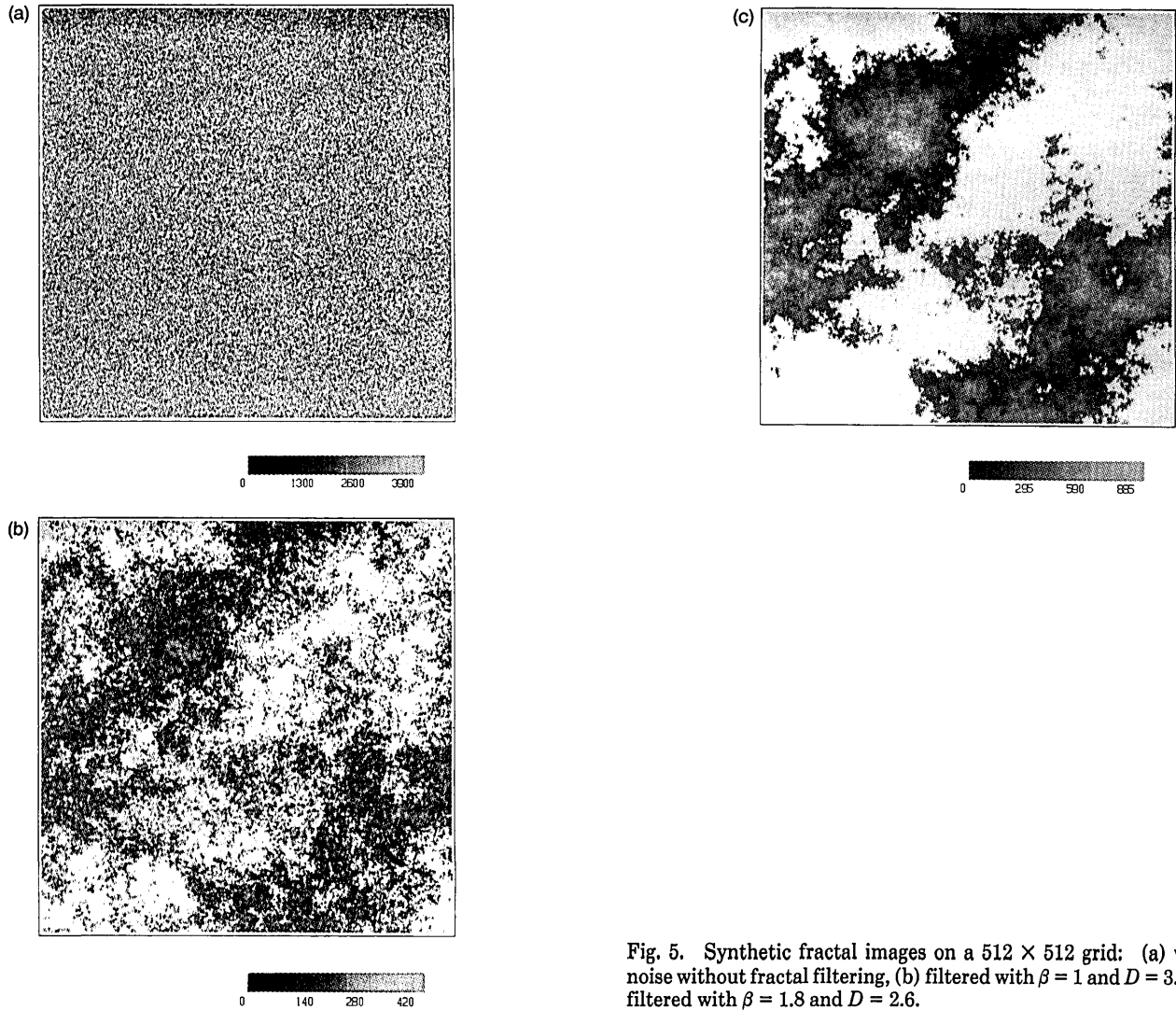

Fig. 5. Synthetic fractal images on a 512 × 512 grid: (a) white noise without fractal filtering, (b) filtered with $\beta = 1$ and $D = 3.0$, (c) filtered with $\beta = 1.8$ and $D = 2.6$.

4(b) is much more impressive. The sedimentary Willamette lowland shows low overall roughness, while the erosional system associated with the nearby mountain ranges and the Wallowa mountains in the northeast stand out as regions of high roughness. The roughness contrasts in the southern basin and range region are also quite remarkable. The fractal analysis gives a quantitative measure of roughness.

FRACTAL ANALYSIS OF SYNTHETIC IMAGES

It is also of interest to generate synthetic fractal maps that can be compared with actual maps. The synthetic map is generated in a square region composed of pixels. The synthetic fractal image is generated as follows:

(1) Each pixel is given a random number based on a Gaussian probability distribution:

$$p(y)dy = \frac{1}{(2\pi)^{1/2}} e^{-y^2/2} dy. \tag{21}$$

(2) Using Eq. (14), we obtain a set of two-dimensional Fourier coefficients H_{st} from the N^2 set of random values given above.

(3) A fractal dimension D_2 is specified, and the corresponding value for β is obtained from Eq. (20). A new set of complex coefficients are obtained from the relation

$$H_{st}^* = H_{st}/k_{st}^{\beta/2}. \tag{22}$$

(4) An inverse two-dimensional Fourier transform is carried out to generate a new image.

Three examples of synthetic images are given in Fig. 5. In Fig. 5(a) the original random data are given without fractal filtering. This is white noise so that $\beta = 0$. In Fig. 5(b) the result is given for $\beta = 1$ ($D = 3.0$) and in Fig. 5(c) for $\beta = 1.8$ ($D = 2.6$). The synthetic result for $D = 2.6$ looks quite realistic for a typical topographic map. This result is consistent with our fractal mapping of the state of Oregon, for which we found the mean fractal dimension to be $D = 2.586$.

We have also carried out one-dimensional spectral decompositions of linear profiles of our synthetic data in the same format as our one-dimensional analysis for Oregon data. The results for synthetic topography with $D = 2.6$, 2.7, and 3.0 are given in Table 2. For realistic topography with $D = 2.6$–2.7, we find that the corresponding one-dimensional profiles give $D = 1.58$–1.65. This result is consistent with the previously published results for one-dimensional bathymetric and topographic profiles for which values near $D = 1.5$ have been found as discussed above. Again, it is close to our results for Oregon for which we found that the mean fractal dimension associated with one-dimensional spectral decompositions is $D = 1.487$.

CONCLUSIONS

We have developed a technique for two-dimensional fractal analysis of digitized topography. Given a digitized data set that exhibits fractal behavior, the texture of the data can be quantitatively analyzed in terms of the fractal dimension and roughness amplitude. We have demonstrated the approach by using the digitized topography of the state of Oregon. The map of roughness amplitude shows considerable variation and provides information on geological and geomorphic processes. We find that the mean two-dimensional fractal dimension for the topography of Oregon is $D = 2.586$. We have also obtained the mean one-dimensional fractal dimension for the topography of Oregon and have found that $D = 1.487$. Thus the one- and two-dimensional fractal dimension approximately differ by unity.

Synthetic two-dimensional images for a range of D values are also generated. We find that for a synthetic image with $D = 2.6$, the corresponding one-dimensional spectral decomposition gives $D = 1.58$. This is consistent with our results for the topography of Oregon and with the results of previous investigations. A number of authors have shown that one-dimensional spectral analyses of topography or bathymetry give fractal dimensions near $D = 1.5$, corresponding to Brown noise.[13] Thus our results are consistent with those of previous authors. It should be emphasized that this technique can be applied to any digitized image that satisfies fractal statistics. The results are generally expected to have a similar pattern to those given here. The fractal dimension is expected to have limited variability, whereas the roughness amplitude is a sensitive measure of texture.

ACKNOWLEDGMENTS

The preparation of this paper has been supported by grant NAG 5-319 from the National Aeronautics and Space Administration. This paper is contribution 850 of the Department of Geological Sciences, Cornell University.

REFERENCES

1. B. Mandelbrot, "How long is the coast of Britain? Statistical self-similarity and fractional dimension," Science **156,** 636–638 (1967).
2. B. Mandelbrot, *The Fractal Geometry of Nature* (Freeman, San Francisco, Calif., 1982).
3. B. Mandelbrot, "Stochastic models for the Earth's relief, the shape and the fractal dimension of the coastlines, and the number-area rule for islands," Proc. Natl. Acad. Sci. USA **72,** 3825–3828 (1975).
4. D. L. Turcotte, "Fractals and fragmentation," J. Geophys. Res. **91,** 1921–1926 (1986).
5. K. Aki, "A probabilistic synthesis of precursory phenomena," in *Earthquake Prediction,* D. W. Simpson and P. G. Richards, eds. (American Geophysical Union, Washington, D.C., 1981), pp. 566–574.
6. D. L. Turcotte, "Fractals in geology and geophysics," Pure Appl. Geophys. **131,** 171–196 (1989).
7. M. F. Goodchild, "Fractals and the accuracy of geographical measures," Math. Geol. **12,** 85–98 (1980).
8. B. Mandelbrot, "Self-affine fractal sets, I: the basic fractal dimensions," in *Fractals in Physics,* L. Pietronero and E. Tosatti, eds. (Elsevier, Amsterdam, 1986), pp. 3–15.
9. R. F. Voss, "Random fractals: characterization and measurement," in *Scaling Phenomena in Disordered Systems,* R. Pynn and A. Skjeltrop, eds. (Plenum, New York, 1985), pp. 1–11.
10. R. F. Voss, "Random fractal forgeries," in *Fundamental Algorithms for Computer Graphics,* Vol. F17 of NATO ASI Series, R. A. Earnshaw, ed. (Springer-Verlag, Berlin, 1985), pp. 805–835.
11. C. Cox and H. Sandstrom, "Coupling of internal and surface waves in water of variable depth," J. Oceanogr. Soc. Jpn. **20,** 499–513 (1962).
12. F. P. Bretherton, "Momentum transport by gravity waves," Q. J. R. Meteorol. Soc. **95,** 213–243 (1969).

13. B. A. Warren, "Transpacific hydrographic sections at lats. 43° S and 28° S: the SCORPIO Expedition. II. Deep water," Deep-Sea Res. **20,** 9–38 (1973).
14. T. H. Bell, "Statistical features of sea-floor topography," Deep-Sea Res. **22,** 883–892 (1975).
15. T. H. Bell, "Mesoscale sea floor roughness," Deep-Sea Res. **26A,** 65–76 (1979).
16. G. I. Barenblatt, A. V. Zhivago, Y. P. Neprochnov, and A. A. Ostrovskiy, "The fractal dimension: a quantitative characteristic of ocean-bottom relief," Oceanology **24,** 695–697 (1984).
17. C. G. Fox and D. E. Hayes, "Quantitative methods for analyzing the roughness of the seafloor," Rev. Geophys. **23,** 1–48 (1985).
18. D. Gilbert and V. Courtillot, "Seasat altimetry and the South Atlantic geoid, I. Spectral analysis," J. Geophys. Res. **92,** 6235–6248 (1987).
19. G. Balmino, K. Lambeck, and W. M. Kaula, "A spherical harmonic analysis of the Earth's topography," J. Geophys. Res. **78,** 478–481 (1973).
20. D. L. Turcotte, "A fractal interpretation of topography and geoid spectra on the Earth, Moon, Venus, and Mars, in *Proceedings of the Lunar Planetary Science Conference 17, Part 2,* J. Geophys. Res. **92** suppl., E597–E601 (1987).
21. R. F. Voss, "Fractals in nature: from characterization to simulation," in *The Science of Fractal Images,* H. Peitgen and D. Saupe, eds. (Springer-Verlag, New York, 1988), pp. 21–70.
22. J. Huang and D. L. Turcotte, "Fractal mapping of digitized images: application to the topography of Arizona and comparisons with synthetic images," J. Geophys. Res. **94,** 7491–7495 (1989).